# Electronic Supplementary Information

## Toward Low-Emissivity Passive Heating: A Supramolecular-Enhanced Membrane with Warmth Retention

Leqi Lei[a], Dong Wang[ab], Shuo Shi[a], Jieqiong Yang[a], Jing Su[b], Cong Wang,[a] Yifan Si,[a] Jinlian Hu*[a]

[a] Department of Biomedical Engineering, City University of Hong Kong, Kowloon, Hong Kong.

[b] Key Laboratory of Eco-Textile, College of Textiles and Clothing, Jiangnan University, 1800 Lihu Road, Wuxi, Jiangsu 214122, China.

*** Corresponding Author**

E-mail: jinliahu@cityu.edu.hk

**Electronic Supplementary Information Includes:**

**1: Experimental Procedures.**

**2: Fig. S1～Fig. S9.**

**3: Table. S1.**

## Experimental Procedures

**Materials:** Polyurethane (PU) was supplied by Shanghai Huntsman Polyurethanes Specialties Co., Ltd., China. Polyvinylidene Difluoride (PVDF) was obtained from Dongguan Zhanyang Polymer Materials Co., Ltd., China. Dimethylformamide (DMF) and Lithium Chloride (LiCl) were purchased from Sinopharm Chemical Reagent Co., Ltd., China. Lithium fluoride (LiF, 99.9%) was obtained by Shanghai Macklin Biochemical Co., Ltd., China. Hydrochloric acid (HCl, 37 wt%) was provided by Shanghai Aladdin Biochemical Co., Ltd., China. MAX-$Ti_3AlC_2$ (98% purity, 400 mesh) powders were purchased from Jinlin 11 Technology Co., Ltd., China.

**Synthesis of $Ti_3C_2T_x$ MXene nanosheets:** A procedure called selective etching is used to synthesize delaminated MXene.[36] Briefly, 1.0 g of LiF was added to 20 mL of HCl (9 mol/L) to obtain an etching solution, followed by the addition of 1.0 g $Ti_3AlC_2$ MAX powder to aforementioned solution. The mixed solution was stirred vigorously for 24 h at 35 °C. Subsequently, the resultant sediment after centrifugation was washed until the pH of the solution reached 6. The precipitate undertook ultrasonic treatment for 1 h, followed by centrifugation for 1 h. Finally, a powder of MXene nanosheets was obtained after the dry-frozen process.

**Preparation of PVDF or/and PU electrospun membrane:** First, 18g DMF organic solution was violently dispersed in a flask, then 2g PVDF powder was slowly added into the DMF solution with vigorous stirring, and then, 0.1 g LiCl was also added to enhance the continuous process of electrospinning technology. The same procedure was conducted, and the same chemicals were utilized except for powder of PU (2g) and polyblend (PVDF(1g) and PU(1g)) instead of PVDF powder. For the electrospinning process, a 10 mL plastic syringe containing a homogenous polymer solution (10 Wt%)

was utilized, along with an applied voltage of 20 kV and a syringe speed rate of 1 mL $h^{-1}$. A distance of 15 cm was selected between the rolling collector and the syringe needle.

**Fabrication of SupraEMs：** Before-mentioned electrospun membranes of PVDF, PU, PVDF&PU were further incorporated with 20mL MXene colloidal solution (2 mg/mL) via vacuum filtration procedure, labeled as PVDF/MXene, PU/MXene, PVDF&PU/MXene, respectively. Finally, SupraEMs were obtained based on the different polymer substrates.

**Characterization and Measurement:** Characterizations were measured by TEM (Talos F200S G2 TEM, America) and SEM (U8100 (Regulus8100), Hitachi, Japan), including surface and cross-section. The phase structure and elemental valence of nanocomposites were investigated by XRD (D2 PHASER, Bruker AXS, Germany) and X-ray photoelectron spectrometer (Axis Ultra DLD, Kratos, UK) with an Al K X-ray source (hv = 1486.6 eV). All thermal images were captured by infrared thermography (TESTO 871, Germany) ranging from 30 °C to 35 °C. Fourier transform infrared spectroscopy, FTIR, (Nicolet 6700, Thermo Scientific, USA) was employed. Applied with an FTIR spectrometer (Spotlight 200i, PerkinElmer) equipped with infrared integrating sphere attachment. The water vapor transmission (WVT) was measured with the standard of ASTM E96 by employing Haida International Equipment (Model-HD-E702-100-4, Dongguan, China). The tensile testing machine (AGS-X-50N, Shimadzu Japanese) was applied to measure the breaking strength and elongation of a single-layer fiber film. Thermogravimetric analysis was performed to evaluate the thermal oxidation resistance by a thermaonalyzer instrument (TGA2, Mettler-Toledo,

Switzerland) at 30–700 °C with an $N_2$ flow of 20 mL·min$^{-1}$. The specific heat capacity was measured by a differential scan calorimeter (DSC, Q200, TA Instruments Inc., New Castle, DE).

**Theoretical Computation:** All the DFT calculations were carried out with the Dmol3 module in Materials Studio software.[1] Perdew-Burke-Ernzerh (PBE) parametrization of the generalized gradient approximation (GGA) was applied as the exchange-correlation functional, which has been shown to be effective for describing the long-range van der Waals (vdW) interaction correction in all computations.[2,3] The self-consistent field (SCF) tolerance was moderate accuracy quality in the intrinsic system, while k-point mesh was set as 2 × 2 × 1 to optimize $Ti_3C_2T_x$ surface (001), and the cutoff energy was set as 520 eV, the criteria of convergence for maximum force, energy, and displacement were 0.004 eV/ Å, $2\times10^{-5}$ eV, and 0.005 Å, respectively. A vacuum layer with a minimum 20 Å thickness was utilized to prevent unintended interactions between adjacent picture cells. The adsorption energy E of MXene was described as:

$$E = E_{total} - E_{surface} - E_{MXene} \quad [1]$$

where $E_{total}$, $E_{surface}$, and $E_{MXene}$ represent the as-calculated energies based on DFT of the surface with adsorbed MXene, Pure surface, and MXene molecule, respectively. The more negative value of $E_{ad}$ implies superior absorption capacity.

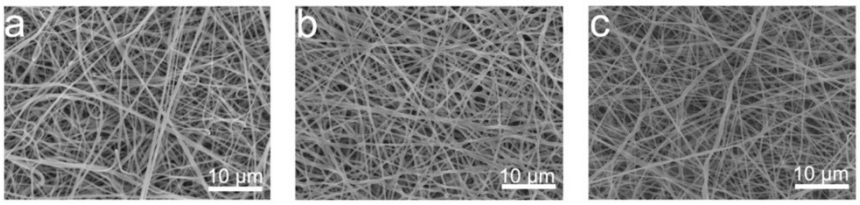


**Fig. S1** SEM images of (a) PVDF, (b) PU, and (c) PVDF&PU on a 10μm scale bar.

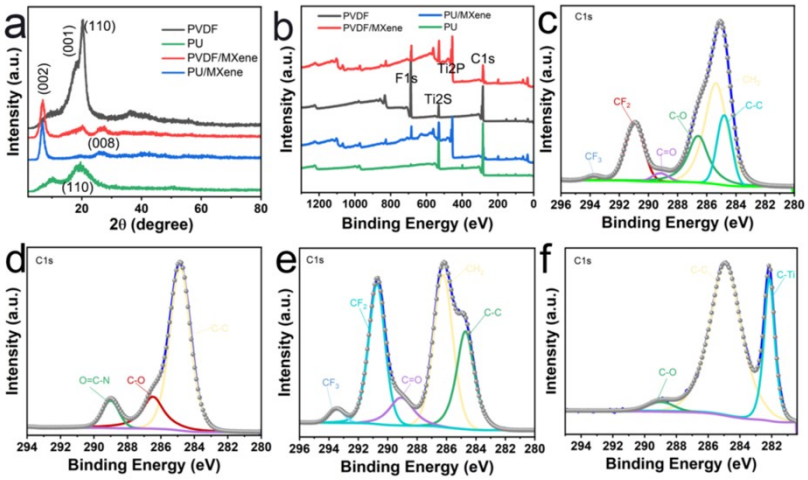


**Fig. S2** (a) FTIR spectra, and (b) XPS survey spectra of various samples. C 1s high-resolution spectra of the (c) PVDF, (d) PU, (e) PVDF&PU, and (f) PVDF&PU/MXene.

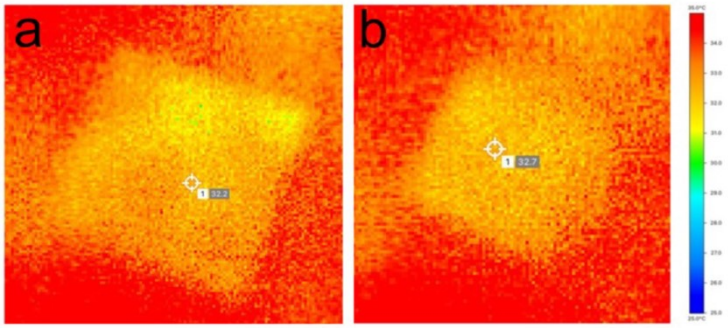


**Fig. S3** Infrared camera images of (a) PVDF, and (b) PU

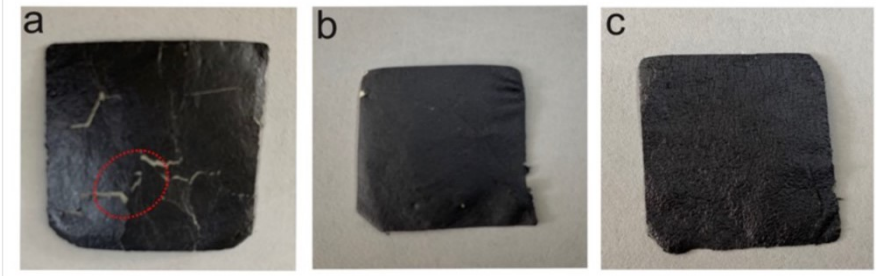


**Fig. S4** Photographs of PVDF&PU (g) PVDF/MXene, (h) PU/MXene, and (i) PVDF&PU/MXene.

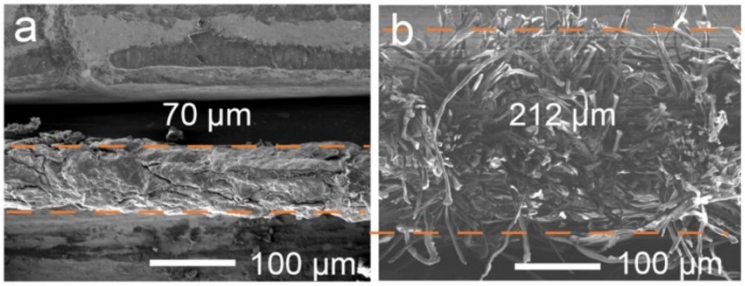


**Fig. S5** SEM images of (a) PVDF&PU/MXene, (b) Cotton

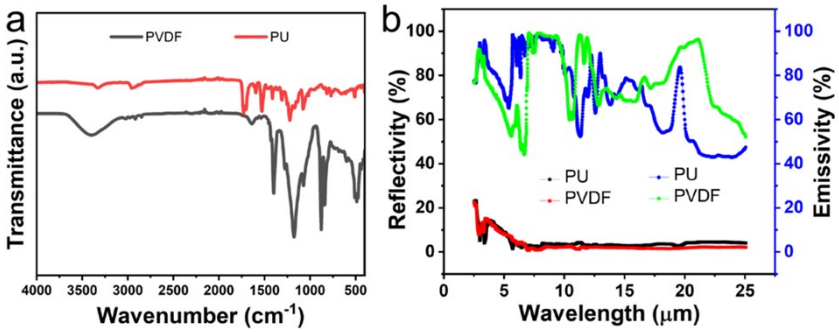


**Fig. S6** (a) FTIR spectra, and (b) Reflectivity and emissivity of PVDF and PU samples.

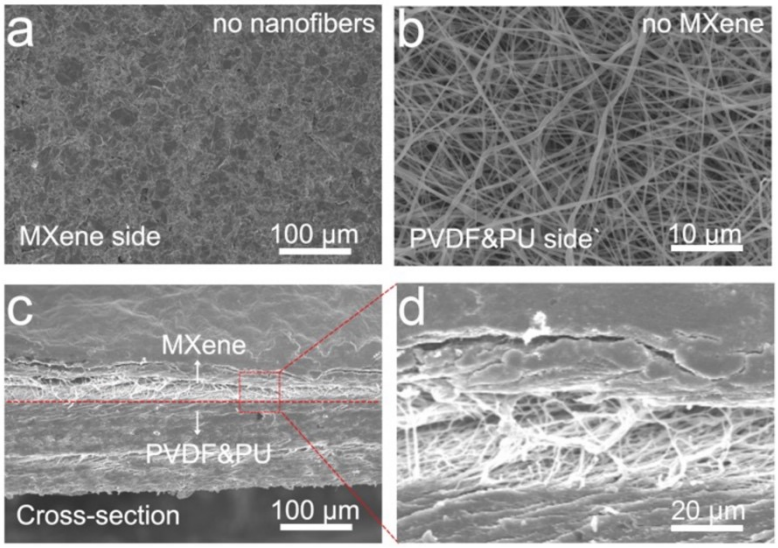


**Fig. S7** SEM images of PVDF&PU/MXene (a) MXene side. (b) PVDF&PU side. (c) Cross-section. (d) High magnification of cross-section.

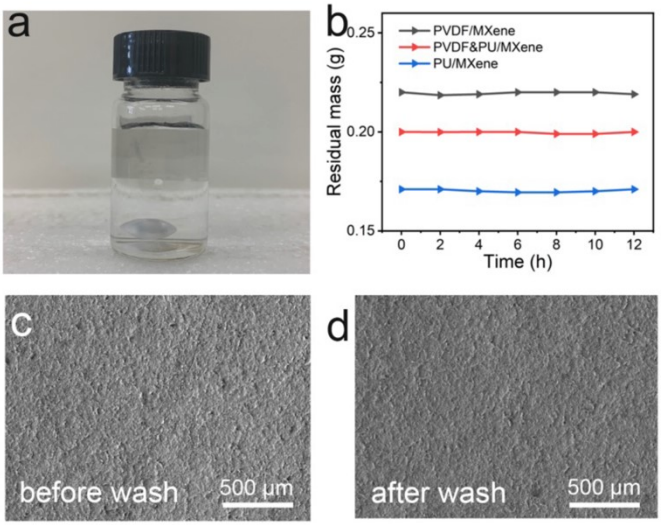


**Fig. S8** Wash resistance test. (a) The photograph of PVDF&PU/MXene after vigorously stirring 12 hrs. (b) Residual mass of MXene-decorated membrane with processing different stirring time. SEM images of PVDF&PU/MXene surface (c) Before wash resistance test and (d) After wash resistance test.

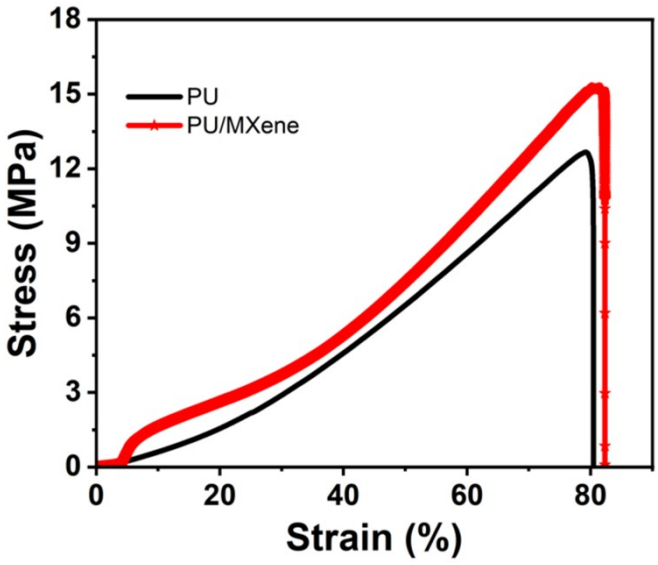


**Fig. S9** Mechanical properties of PU and PU/MXene.

**Table 1.** List of the thermal efficiency and wearability of recently reported state-of-the-art thermoregulatory textiles, and our demonstrated SEM.

| Materials | Emissivity | Warming Retention (°C) | WVT (kg $m^{-2}$ $d^{-1}$) | Stress (MPa) | Ref. |
|---|---|---|---|---|---|
| PVDF&PU/MXene | 0.246 | 6.2 | 11.6 | 12 | This work |
| Cloth/AgNW | 0.592 | 0.9 | - | - | 4 |
| NanoPAN/Ag | 0.15 | 2 | 8.49 | 8.2 | 5 |
| Cu/$MnO_2$/Cellulose@LDH | 0.436 | 2.1 | 2.64 | - | 6 |
| AgNPs/Cellulose | - | 2.0 | - | - | 7 |
| Ag/Si | 0.3 | 2.3 | 3.22 | - | 8 |
| CuNWs/cotton | - | 0.5 | - | - | 9 |
| Ni-Al-LDH/ICM | 0.054 | 1.7 | 0.66 | - | 10 |
| PCMF | 0.231 | 2.5 | - | 5.5 | 11 |
| PTFE | 0.175 | 2.3 | - | 3 | 12 |

# References


1 S. Grimme, J. Antony, S. Ehrlich and H. Krieg, *J. Chem. Phys.*, 2010, **132**, 154104.

2 J. P. Perdew, K. Burke and M. Ernzerhof, *Phys. Rev. Lett.*, 1996, **77**, 3865–3868.

3 Y. Zhao and D. G. Truhlar, *J. Chem. Phys.*, 2006, **125**, 194101.

4 P.-C. Hsu, X. Liu, C. Liu, X. Xie, H.R. Lee, A.J. Welch, T. Zhao, Y. Cui, Nano Lett., 2015,**15**, 365–371.

5 X. Li, Y. Yang, Z. Quan, L. Wang, D. Ji, F. Li, X. Qin, J. Yu, S. Ramakrishna, Chem. Eng. J., 2022, **430**, 133093.

6 X. Yue, T. Zhang, D. Yang, F. Qiu, G. Wei, H. Zhou, Nano Energy, 2019, **63**, 103808.

7 B. Gu, K. Liang, T. Zhang, X. Yue, F. Qiu, D. Yang, M. Chen, Cellulose, 2019, **26**, 8745–8757.

8 Q. Hu, J. Huang, J. Wang, R. Tan, Y. Feng, X. Xu, J. Li, Y. Lu, W. Song, J. Mater.

Sci., 2022, **57**, 11477–11490.

9 Z. Guo, C. Sun, J. Wang, Z. Cai, F. Ge, ACS Appl. Mater. Interfaces, 2021, **13**, 8851–8862.

10 B. Gu, H. Zhou, Z. Zhang, T. Zhang, M. Chen, F. Qiu, D. Yang, Appl. Surf. Sci., 2021, **535**, 147670.

11 J. Wu, R. Hu, S. Zeng, W. Xi, S. Huang, J. Deng, G. Tao, ACS Appl. Mater. Interfaces, 2020, **12**, 19015–19022.

12 Y. Zhang, Y. Li, K. Li, Y.S. Kwon, T. Tennakoon, C. Wang, K.C. Chan, S.-C. Fu, B. Huang, C.Y.H. Chao, Nano Energy, 2022, **95**, 106996.